Quantum Clusters

$Au_{25}@SiO_2$: Quantum Clusters of Gold Embedded in Silica

*M. A. Habeeb Muhammed and T. Pradeep**

Quantum clusters (QC) or subnanoclusters of noble metals constitute a relatively new class of nanomaterials with molecular cores composed of a few atoms. Their electronic structure and physicochemical properties are totally different from metallic nanoparticles of the same element. They possess discrete electronic energy levels and show 'molecule-like' optical transitions in absorption and emission. Even though they are relatively new, several methods have been developed to synthesize both aqueous[1–7] and organic[9–11] soluble QCs. Several of their properties, especially photoluminescence, have been exploited. Two-photon-induced emission,[3a] photon antibunching,[1b] room-temperature electroluminescence,[3b] and fluorescence resonance energy transfer (FRET)[3c] have been reported in them. They find applications in areas such as cancer-cell imaging,[2] catalysis,[11] and the creation of fluorescent patterns,[6] amongst others. Among the various QCs synthesized so far, Au_{25} is widely explored due to its extraordinary stability.[4] Various methods have been developed for the synthesis of Au_{25}.[4,5,7,8d,13] However, the main drawbacks of the synthetic methods, especially for water-soluble Au_{25}, are low yield and long reaction times. The clusters are also reactive[5a] and unstable in diverse media. Confinement of QCs in oxides such as silica may provide them with additional stability. At the same time, such protection imparts additional functionality and hence additional properties. Silica protection of various nanostructures, such as nanoparticles, nanorods, and so on, has been studied extensively[15] and such a possibility will provide new attributes to QCs, as in the case of nanoparticles.[16]

In this Communication, we present a rapid method to synthesize monodisperse water-soluble Au_{25} from polydisperse glutathione (GSH, bound to gold in the thiolate form, SG)-protected gold QCs (Au_mSG_n) by reaction with (3-mercaptopropyl)trimethoxysilane (MPTS). It is known that only certain ligands result in the formation of QCs. The reason for this selectivity is unknown owing to the limited knowledge of QC growth. Until now, only GSH has been known to assist the synthesis of water-soluble Au_{25} with characteristic optical absorption features.[4,5] Even the synthesis of Au_{25} with *N*-acetyl/*N*-formyl derivatives of glutathione was unsuccessful.[5b] The advantages of MPTS-mediated Au_{25} synthesis over GSH-mediated synthesis are shorter reaction times. the absence of Au(I)thiolate by-product, and hence high yield, and room-temperature reaction. Subsequent hydrolysis and condensation resulted in the formation of $Au_{25}@SiO_2$, where the QCs are embedded in a layer of silica.

Water-soluble Au_mSG_n QCs were prepared by the reduction of Au^{3+} ions in presence of GSH at 0 °C. This method produced a highly polydisperse solution containing QCs of different chemical compositions, ranging from $Au_{10}SG_{10}$ to $Au_{39}SG_{24}$.[4a,c] To start the synthesis of Au_{25} QCs, MPTS was added to the aqueous solution of Au_mSG_n having a pH of 6–7. The solution was stirred at room temperature and the progress of the reaction was monitored by measuring the optical-absorption spectrum of the solution at regular intervals. The formation of Au_{25} took only 1–10 min. The QC produced by this method is referred to as Au_{25}@MPS hereafter, where MPS corresponds to (3-mercaptopropyl)trisilanol (the reason for this name will be described later). In contrast, GSH-mediated Au_{25} ($Au_{25}SG_{18}$) synthesis from Au_mSG_n took 3–12 h.[4c,5,6] Once Au_{25}@MPS is formed, it is possible to grow a thin silica layer on the QC surface since the cluster has silanol protection. The monolayers were subjected to hydrolysis and condensation at basic pH. The pH of the aqueous solution of QC was adjusted to 12 and the solution was heated at 65 °C for 30 min. On the other hand, during acid-mediated hydrolysis, the QCs settled down immediately due to aggregation. Au_{25}@MPS after hydrolysis and condensation will be designated as $Au_{25}@SiO_2$ hereafter.

The optical absorption spectrum of Au_mSG_n was almost featureless (trace 'a' of **Figure 1**) due to the polydispersity as well as the subnanometer core size of the QCs. However, the spectrum of Au_{25} is molecule-like with distinct features assigned to molecular transitions,[9e] in sharp contrast to that of metallic gold nanoparticles, and it is possible to identify this QC from these features alone. A typical absorption spectrum of Au_{25} has several distinct absorption peaks, three of them appear pronounced around 670–690, 450, and 400 nm; the spectrum of $Au_{25}SG_{18}$ is shown in Figure S1 of the Supporting Information (SI).[9e,4,5] The first absorption peak (labeled as '*peak 1*' in Figure S1 of the SI) corresponds to a highest occupied molecular orbital (HOMO)–lowest occupied molecular orbital (LUMO) transition, which is otherwise referred to as an intraband (sp to sp) transition. The second peak (*peak 2*) arises from mixed intraband (sp to sp) and interband (d to sp) transitions. The third peak (*peak 3*) arises from an interband transition (d to sp). For Au_{25}@MPS, these features appeared at 700, 455, and 400 nm, respectively, which are indicated in Figure 1. $Au_{25}SG_{18}$ exhibited *peak 1* at

M. A. Habeeb Muhammed, Prof. T. Pradeep
Department of Chemistry
Indian Institute of Technology Madras, 600036, India
E-mail: pradeep@iitm.ac.in

DOI: 10.1002/smll.201001332

small NANO MICRO

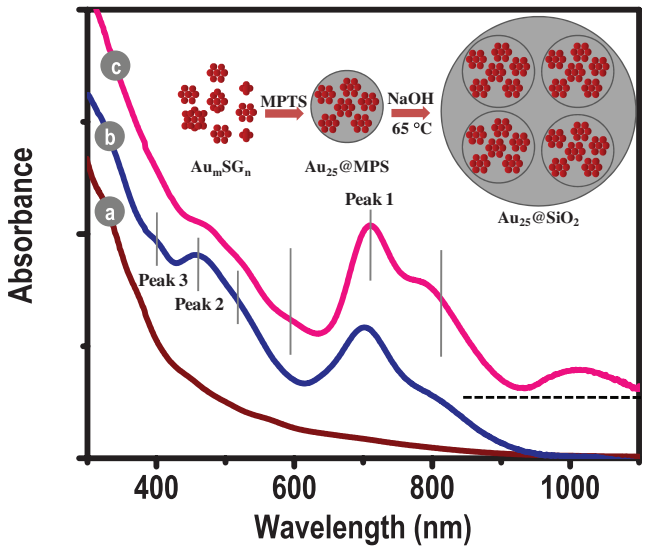

Figure 1. Optical absorption spectra of a) Au_mSG_n, b) Au_{25}@MPS, and c) Au_{25}@SiO_2. The features of the QCs are indicated with lines (see the text for explanation).

670 nm (Figure S1 of the SI). On the other hand, *peak 1* of Au_{25}@MPS showed a redshift of ≈30 nm. A redshift in *peak 1* is observed when the ligand chemistry and/or refractive index of the medium changes. For example, *peak 1* showed a redshift of 10 nm when some of the GSH ligands were exchanged with mercaptobutanol (MB).[5b] On the other hand, there was no shift when the GSH ligand was exchanged with its acetyl and formyl derivatives.[5b] In these cases, the chemical environment surrounding the QC is more or less the same when compared with the parent $Au_{25}SG_{18}$. These studies propose that the redshift in *peak 1* is likely when the chemical environment is changed. The other two prominent features of Au_{25}@MPS at 455 and 400 nm are close to the positions seen in $Au_{25}SG_{18}$ (Figure S1 of the SI). There are three other features around 501, 560, and 785 nm in $Au_{25}SG_{18}$, of which the first and third features appear around 518 and 815 nm for Au_{25}@MPS. The QC retained its optical absorption features after hydrolysis and condensation also with a 7-nm shift in *peak 1*. All the features of Au_{25} are clear in trace 'c', including the feature at ≈580 nm, which is masked in Au_{25}@MPS. These QCs showed a broad near-infrared (NIR) peak centered around 1015 nm, which may be attributed to intercluster interactions within the aggregates.

Transmission electron microscopy (TEM) of Au_mSG_n showed polydisperse QCs as expected due to the presence of several clusters (Figure S2 of the SI). On the other hand, Au_{25}@MPS showed spherical cluster aggregates of ≈20 nm in size throughout the TEM grid (see **Figure 2**A). Each such aggregate is composed of QCs of ≈1-nm core size (Figure 2B). No individual QCs were seen in the images. $Au_{25}SG_{18}$ shows well separated Au_{25} with a core size of ≈1 nm (inset of Figure S2 of the SI). Thus, TEM supports the existence of Au_{25} clusters within the aggregates. These aggregates exhibit an average hydrodynamic diameter of 35 nm in solution (Figure S3). There were no other peaks in the dynamic light-scattering (DLS) data, which confirm that the solution contains uniformly sized spherical aggregates of Au_{25}@MPS. Thus, the 30-nm shift in *peak 1* is due to the change in the ligand nature and aggregate formation. TEM analysis of Au_{25}@SiO_2 showed the growth of a silica layer. A representative large-area image is shown in **Figure 3**A. An expanded image (Figure 3B) further shows that the QCs are embedded in a layer of silica. A layer projecting out of the grid with embedded clusters is shown in the inset of Figure 3B. The aggregates of Au_{25}@SiO_2 are larger than Au_{25}@MPS and contain more clusters on an average, which may be the reason for the occurrence of the NIR feature in the UV/vis spectrum. However, well separated Au_{25} with silica shell was not observed.

To prove the MPS protection of Au_{25}, Fourier-transform infrared (FTIR) spectroscopy, X-ray photoelectron spectroscopy (XPS), and energy-dispersive analysis of X-rays (EDAX) were performed. The FTIR spectrum of Au_{25}@MPS was compared with that of MPTS used for reaction (Figure S4A of the SI). The band at 2565 cm^{-1} due to the –S–H stretching of MPTS was absent in Au_{25}@MPS (Figure S4B of the SI) suggesting Au–S covalent bonding between the Au_{25} core and MPTS ligand.[12] While the spectrum of MPTS showed bands that are typical for methoxysilane groups (Si–O–CH_3) at 2966, 2942, and 2840 cm^{-1}, all these peaks were absent in the Au_{25}@MPS spectrum (Figure S4C of the SI). There is a band of Si–OH at 947 cm^{-1} in the Au_{25}@MPS spectrum and this band was absent for MPTS (Figure S4D of the SI). The last two observations suggest the hydrolysis of silane ligands on the Au_{25} surface to silanol and hence the resulting cluster is described as Au_{25}@MPS. Bands typical of extended Si–O–Si bonds are absent. The peaks due to –CH_2 stretching were present both in MPTS and Au_{25}@MPS (Figure S4C of the SI). In order to understand the chemical composition, Au_mSG_n and Au_{25}@MPS were analyzed by XPS (Figure S5 of the SI). XPS of Au_mSG_n showed the presence of Au, C, O, N, and S. As Au_mSG_n was protected with GSH ($C_{10}H_{17}N_3O_6S$),

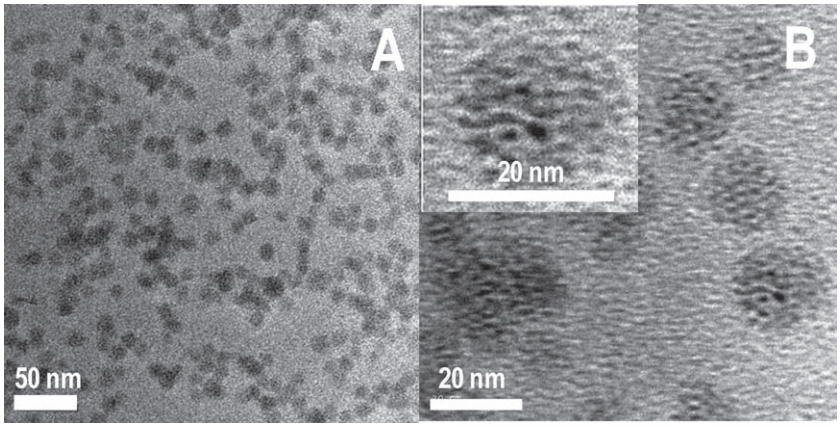

Figure 2. A) Low- and B) high-magnification TEM images of Au_{25}@MPS. A portion of (B) is expanded in the inset.

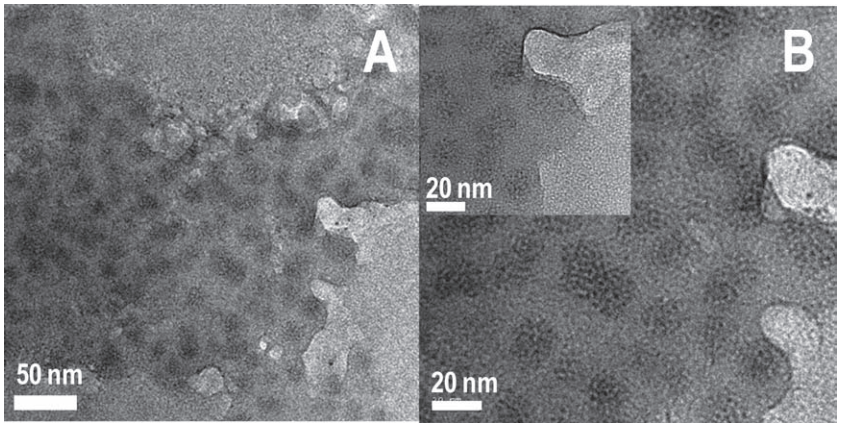

Figure 3. A) Low- and B) high-magnification TEM images of Au_{25}@SiO_2. A portion of (B) is expanded in the inset.

the presence of these elements in the spectrum is justified. On the other hand, XPS of Au_{25}@MPS showed the presence of Au, C, O, S, and Si, in view of the capping of MPS ($C_3H_{10}O_3SSi$). The absence of N in Au_{25}@MPS is due to the complete coverage of the QC by MPS and because all the –SG ligands are exchanged by MPS during the course of the reaction (Figure S5E of the SI). Note that there is no nitrogen in MPS. The presence of Si in the QCs also confirms the MPS protection. Si 2p is absent in Au_mSG_n, as expected (Figure S5B of the SI). In order to check the presence of gold and other elements in the entire sample, EDAX was carried out (Figure S6 of the SI). The elements present in the QC were Au, C, O, S, and Si and they were mapped.

X-ray powder diffraction (XRD) of Au_{25}@MPS showed a broad diffraction peak at $2\theta \approx 35°$ for the QC (Figure S7 of the SI). This is similar to the (111) plane of bulk gold and indicates the cubic packing of atoms in the cluster. The QCs are too small to possess all the peaks of bulk gold. A similar peak was observed for $Au_{20}(CH_2CH_2Ph)_{16}$.[9b] Quantum clusters exhibit luminescence with varying quantum yield. Au_{25}@MPS showed an emission maximum at 740 nm (Figure S8 of the SI) when excited at 530 nm. The emission is due to excitation across the HOMO–LUMO gap. On the other hand, the emission maximum of $Au_{25}SG_{18}$ is at 700 nm when excited at the same wavelength.[2b,3c,5] Photoluminescence profiles of Au_{25}@MPS and $Au_{25}SG_{18}$ are compared in Figure S8 of the SI. The shift in emission wavelength can be attributed to the change in ligand chemistry as well as aggregation, as discussed earlier. The photoluminescence profile is similar to that of $Au_{25}SG_{18}$.[2b,3c,5] Au_{25}@MPS is also luminescent in the solid state (Figure S9 of the SI). The clusters can be imaged using their inherent fluorescence. Fluorescence image of Au_{25}@MPS in powder form was recorded using a confocal Raman spectrometer equipped with 532-nm excitation. In the image, while there was luminescence from the red spots, there was no luminescence from the dark areas. The red spots are the islands of the clusters.

The yield of Au_{25} formed by MPTS-mediated synthesis is ≈7 times higher than that of GSH-mediated synthesis. To prove this, equal amounts of Au_mSG_n, dissolved in equal amounts of water were treated with optimized concentrations of GSH and MPTS, separately (these concentrations gave highest yields). The absorbance of *peak 1* was measured after the QC formation to determine the concentration of the Au_{25} in the solution. The absorbance of Au_{25}@MPS was ≈7 times higher when compared with that of $Au_{25}SG_{18}$, as shown in **Figure 4** under identical conditions. Moreover, the by-product, the insoluble Au(I)thiolate, was observed only for GSH-mediated synthesis,[4c,5] which was not formed during MPTS-mediated synthesis (inset of Figure 4). It is known that when excess GSH is added to Au_mSG_n, selective formation of $Au_{25}SG_{18}$ occurs.[4c] Two modes of reaction happened. While the smaller QCs ($m < 25$) were completely oxidized to Au(I)SG thiolates, the bigger QCs ($m > 25$) were etched to form Au_{25} by free GSH molecules. The selective formation of Au_{25} happened due to their extraordinary stability when compared with other QCs. However, for MPTS-mediated synthesis, we did not observe any Au(I)thiolate and the absorbance was also higher. This suggests that all the QCs, from $Au_{10}SG_{10}$ to $Au_{33}SG_{14}$ were converted into Au_{25}. There are reports showing the conversion of smaller QCs, such as Au_{11}, into bigger QCs and vice versa when treated with appropriate ligand.[4b] When MPTS was added to Au_mSG_n, core etching with ligand exchange occurred. Thiols have a tendency to undergo ligand exchange with the already existing ligand on a nanoparticle/QC surface. However, if thiols are added in large quantities, QCs undergo aggregation and dissociation resulting in the selective formation of extraordinarily stable QCs with ligand exchange. The selective formation of Au_{25} supports the earlier reports on the extraordinary stability of Au_{25}.

$Au_{25}SG_{18}$ was found to be very reactive towards $HAuCl_4$ and underwent instantaneous decomposition with the disappearance of the characteristic absorption features due to the core collapse.[5a] On the other hand, Au_{25}@MPS and Au_{25}@SiO_2 were found to be at least five-fold stable in presence of

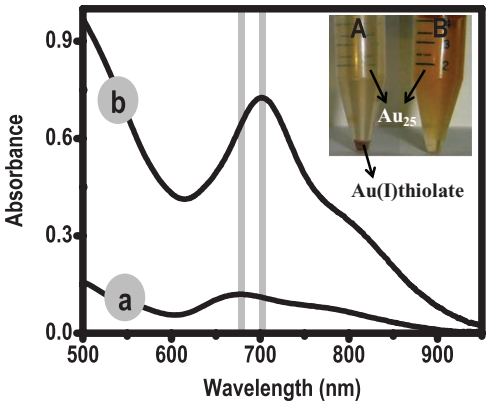

Figure 4. Comparison of the absorbance of *peak 1* of Au_{25} formed by a) GSH- and b) MPTS-mediated syntheses. Inset shows photographs of the reaction products upon reaction with A) GSH and B) MPTS, after centrifugation.

small NANO MICRO

$HAuCl_4$ (measured in terms of concentration needed for complete decomposition), probably due to the silanol/silica protection (data not shown). The QCs are very sensitive towards the electron beam and fuse together to form bigger nanoparticles on prolonged electron-beam irradiation (Figure S10 of the SI).[17] The silica growth greatly enhanced the stability of QCs against electron-beam-induced aggregation.

In summary, a rapid synthesis of monodisperse, water-soluble Au_{25} from polydisperse Au_mSG_n by the addition of MPTS at pH 6 is reported. Until now, only GSH has been known to make water-soluble Au_{25}. The yield of MPTS-mediated Au_{25} synthesis was ≈7 times higher when compared with GSH-mediated synthesis. Subsequent hydrolysis and condensation resulted in the formation of $Au_{25}@SiO_2$, where the QCs are embedded in a layer of silica. This method leads to the production of Au_{25} QCs rapidly with high yield. We believe the silica protection will add several functionalities to the QC as in the case of other nanostructures.

Experimental Section

Synthesis of Glutathione-Protected Gold Clusters: Glutathione-protected gold clusters were synthesized according to a reported method.[9] To $HAuCl_4 \cdot 3H_2O$ (100 mL, 5 mM) in methanol, reduced glutathione (GSH, 614 mg) was added. The mixture was then cooled to 0 °C in an ice bath for 30 min. An aqueous solution of $NaBH_4$ (25 mL, 0.2 M), cooled at 0 °C, was injected rapidly into this mixture under vigorous stirring. The mixture was allowed to react for another 1 h. The resulting precipitate was collected and washed repeatedly with a methanol/water (3:1) mixture through centrifugal precipitation and dried to obtain the Au_mSG_n clusters as a dark-brown powder. This product is a mixture of small nanoparticles and different clusters.

Synthesis of Au_{25} Clusters: Au_{25} clusters were synthesized from the as-prepared Au_mSG_n clusters by a method called preferential population of most-stable cluster. The as-prepared Au_mSG_n clusters were dissolved in water (25 mL). (3-mercaptopropyl)trimethoxysilane was added (20 mM) and stirred at room temperature (28 °C). The reaction was monitored by optical-absorption spectroscopy. The reaction was terminated when the absorption features of Au_{25} clusters appeared in the UV/vis spectrum.

Instrumentation: UV/vis spectra were measured with a Perkin Elmer Lambda 25 instrument in the range of 200–1100 nm. The FTIR spectra were measured with a Perkin Elmer Spectrum One instrument. KBr crystals were used as the matrix for preparing samples. XPS measurements were conducted using an Omicron ESCA Probe spectrometer with monochromatized Mg Kα X-rays ($h\nu$ = 1253.6 eV). A constant analyzer energy of 20 eV was used for the measurements. EDAX was carried out using FEI QUANTA-200 SEM instrument and the samples were prepared on carbon tape. High-resolution TEM measurements were carried out at 200 kV with a JEOL 3010 instrument equipped with a ultrahigh-resolution (UHR) polepiece. The samples were prepared by dropping the dispersion on carbon-coated copper grids and drying in ambient conditions. DLS measurements were performed with Zetasizer 3000HSA (Malvern Instruments, UK). Fluorescence measurements were carried out on a Jobin Yvon NanoLog instrument. The band pass for excitation and emission was set as 5 nm.

Supporting Information

Supporting Information is available from the Wiley Online Library or from the author.

Acknowledgements

We thank Department of Science and Technology (DST), Government of India for constantly supporting our research program on nanomaterials.

[1] a) J. Zheng, J. T. Petty, R. M. Dickson, *J. Am. Chem. Soc.* **2003**, *125*, 7780; b) J. Zheng, P. R. Nicovich, R. M. Dickson, *Annu. Rev. Phys. Chem.* **2007**, *58*, 409.
[2] a) R. Archana, S. Sonali, M. Deepthy, R. Prasanth, Habeeb Muhammed, T. Pradeep, N. Shantikumar, K. Manzoor, *Nanotechnology* **2010**, *21*, 055103; b) M. A. Habeeb Muhammed, P. K. Verma, S. K. Pal, R. C. Arun Kumar, S. Paul, R. V. Omkumar, T. Pradeep, *Chem. Eur. J* **2009**, *15*, 10110.
[3] a) G. Ramakrishna, O. Varnavski, J. Kim, D. Lee, T. Goodson, *J. Am. Chem. Soc.* **2008**, *130*, 5032; b) J. I. Gonzalez, T.-H. Lee, M. D. Barnes, Y. Antoku, R. M. Dickson, *Phys. Rev. Lett.* **2004**, *93*, 147402; c) M. A. Habeeb Muhammed, A. K. Shaw, S. K. Pal, T. Pradeep, *J. Phys. Chem C* **2008**, *112*, 14324.
[4] a) Y. Negishi, K. Nobusada, T. Tsukuda, *J. Am. Chem. Soc.* **2005**, *127*, 5261; b) Y. Shichibu, Y. Negishi, T. Tsukuda, T. Teranishi, *J. Am. Chem. Soc.* **2005**, *127*, 13464; c) Y. Shichibu, Y. Negishi, H. Tsunoyama, M. Kanehara, T. Teranishi, T. Tsukuda, *Small* **2007**, *3*, 835; d) Y. Negishi, Y. Takasugi, S. Sato, H. Yao, K. Kimura, T. Tsukuda, *J. Am. Chem. Soc.* **2004**, *126*, 6518.
[5] a) M. A. Habeeb Muhammed, T. Pradeep, *Chem. Phys. Lett.* **2007**, *449*, 186; b) E. S. Shibu, M. A. Habeeb Muhammed, T. Tsukuda, T. Pradeep, *J. Phys. Chem C* **2008**, *112*, 2168.
[6] E. S. Shibu, B. Radha, P. K. Verma, P. Bhyrappa, G. U. Kulkarni, S. K. Pal, T. Pradeep, *ACS Appl. Mater. Interfaces* **2009**, *1*, 2199.
[7] J. Xie, Y. Zheng, J. Y. Ying, *J. Am. Chem. Soc.* **2009**, *131*, 888.
[8] a) T. G. Schaaff, M. N. Shafigullin, J. T. Khoury, I. Vezmar, R. L. Whetten, *J. Phys. Chem. B* **1997**, *101*, 7885; b) T. G. Schaaff, G. Knight, M. N. Shafigullin, R. F. Borkman, R. L. Whetten, *J. Phys. Chem. B* **1998**, *102*, 10643; c) S. Link, A. Beeby, S. F. Gerald, M. A. El-Sayed, T. G. Schaaff, R. L. Whetten, *J. Phys. Chem. B* **2002**, *106*, 3410; d) R. C. Price, R. L. Whetten, *J. Am. Chem. Soc.* **2005**, *127*, 13750.
[9] a) M. Zhu, E. Lanni, N. Garg, M. E. Bier, R. Jin, *J. Am. Chem. Soc.* **2008**, *130*, 1138; b) M. Zhu, H. Qian, R. Jin, *J. Am. Chem. Soc.* **2009**, *131*, 7220; c) H. Qian, M. Zhu, U. N. Andersen, R. Jin, *J. Phys. Chem. A* **2009**, *113*, 4281; d) H. Qian, M. Zhu, E. Lanni, Y. Zhu, M. E. Bier, R. Jin, *J. Phys. Chem. C* **2009**, *113*, 17599; e) M. Zhu, C. M. Aikens, F. J. Hollander, G. C. Schatz, R. Jin, *J. Am. Chem. Soc.* **2008**, *130*, 5883.
[10] a) G. Wang, R. Guo, G. Kalyuzhny, J.-P. Choi, R. W. Murray, *J. Phys. Chem. B* **2006**, *110*, 20282; b) M. W. Heaven, A. Dass, P. S. White, K. M. Holt, R. W. Murray, *J. Am. Chem. Soc.* **2008**, *130*, 3754.
[11] Y. Zhu, H. Qian, B. A. Drake, R. Jin, *Angew. Chem. Int. Ed.* **2010**, *49*, 1295.
[12] W. R. Thompson, M. Cai, M. Ho, J. E. Pemberton, *Langmuir* **1997**, *13*, 2291.
[13] Z. Wu, J. Suhan, R. Jin, *J. Mater. Chem.* **2008**, *19*, 622.
[14] H. Qian, Y. Zhu, R. Jin, *ACS Nano* **2009**, *3*, 3795.

[15] a) A. Guerrero-Martínez, J. Pérez-Juste, L. M. Liz-Marzán, *Adv. Mater.* **2010**, *22*, 1182; b) I. Pastoriza-Santos, J. Pérez-Juste, L. M. Liz-Marzán, *Chem. Mater.* **2006**, *18*, 2465; c) I. Gorelikov, N. Matsuura, *Nano Lett.* **2008**, *8*, 369.
[16] a) J. F. Li, Y. F. Huang, Y. Ding, Z. L. Yang, S. B. Li, X. S. Zhou, F. R. Fan, W. Zhang, Z. Y. Zhou, D. Y. Wu, B. Ren, Z. L. Wang, Z. Q. Tian, *Nature* **2010**, *464*, 392; b) A. Villanueva, P. de la Presa, V. Alonso, J. M. Rueda, T. Martnez, A. Crespo, P. Morales, M. P. Gonzalez-Fernandez, M. A. Valds, J. G. Rivero, *J. Phys. Chem. C* **2010**, *114*, 1976; c) C. H. Yu, C. C. H. Lo, K. Tam, S. C. Tsang, *J. Phys. Chem. C* **2007**, *111*, 7879–7882.
[17] P. Ramasamy, S. Guha, E. S. Shibu, T. S. Sreeprasad, S. Bag, A. Banerjee, T. Pradeep, *J. Mater. Chem.* **2009**, *19*, 8456.

Received: August 3, 2010
Revised: September 1, 2010
Published online: December 7, 2010

